ACS BIO & MED CHEM Au
AN OPEN ACCESS JOURNAL OF THE AMERICAN CHEMICAL SOCIETY

pubs.acs.org/biomedchemau
Article

Design and Synthesis of Mycophenolic Acid Analogues for Osteosarcoma Cancer Treatment

Patamawadee Silalai, Pimpisa Teeyakasem, Dumnoensun Pruksakorn,* and Rungnapha Saeeng*

Cite This: ACS Bio Med Chem Au 2025, 5, 106−118

Read Online

ACCESS | Metrics & More | Article Recommendations | Supporting Information

ABSTRACT: Mycophenolic acid (MPA), a natural compound, was modified to new MPA analogues via the classical method of silylation and esterification. Their cytotoxicity was evaluated in vitro on four osteosarcoma cancer cell lines (MNNG/HOS, U2OS, 143B, and SaOS-2) and human normal cells (hFOB 1.19). The most potent silicon-containing compound **2d** (R^1 = TPS, R^2 = H) exhibited good cytotoxic activity against all osteosarcoma cancer cell lines with IC_{50} values ranging from 0.64 to 2.27 μM and showing low cytotoxicity against normal cells. Further investigations revealed that compound **2d** (R^1 = TPS, R^2 = H) displayed significant inhibition of IMPDH2 with K_{iapp} 1.8 μM. Furthermore, molecular modeling studies were performed to investigate the binding affinity of **2d** (R^1 = TPS, R^2 = H) which can effectively bind to critical amino acids of three proteins (vascular endothelial growth factor receptor 2; VEGFR-2, cyclin-dependent kinase 2; CDK2, inosine-5′-monophosphate dehydrogenase; IMPDH) involved in cancer therapy. This finding suggests that triphenylsilyl-MPA (TPS-MPA) analogue could serve as a promising starting point for developing new anticancer drugs for osteosarcoma.

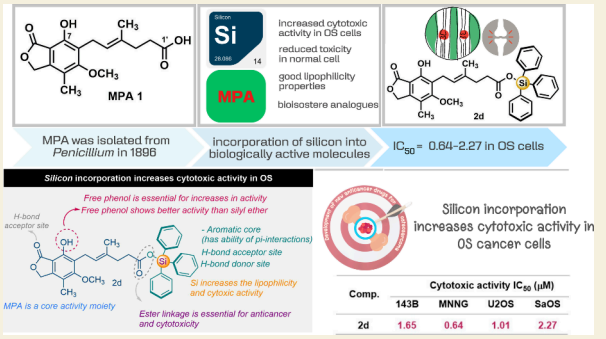

KEYWORDS: *mycophenolic acid, osteosarcoma, cytotoxic activity, molecular docking, silicon*

INTRODUCTION

Osteosarcoma (OS) is a primary malignant bone tumor, and 70% of patients are children and adolescents. Although osteosarcoma is a rare malignancy that accounts for 2−5 patients per million people or 5−6% of all childhood tumors but shows a high predisposition to metastasize distributed from the original site to other organ sites, making it more difficult to cure which is the main cause of cancer-related death.[1,2] Nowadays, the treatment for osteosarcoma consists of chemotherapy and surgical resection.[3] Chemotherapy is an integral approach to cancer therapy.[4] Effective treatment of cancers needs accurate delivery of enough intracellular doses of chemo-drugs to kill the cancer cells and have not spread to normal cells.[5] Recently, the mycophenolate analogues have shown selective cytotoxicity in cancer cells and were less toxic to normal cells in comparison to the lead compound, MPA **1**, and a standard drug, ellipticine.[6]

Mycophenolic acid (MPA) was isolated from *Penicillium* in 1896 by Italian physician Bartolomeo Gosio.[7,8] It comprises a phthalide in which an aromatic ring is substituted with hydroxy, methyl, methoxy, and a six-carbon chain with a double bond in the *E* configuration and the free carboxylic acid.[9] MPA acts as an inhibitor of inosine monophosphate dehydrogenase (IMPDH), a key enzyme in the de novo synthesis of guanine nucleotide that causes the inhibition of lymphocyte activity in humans.[10−12] Therefore, this compound is displayed as an immunosuppressive drug in transplantation to protect against acute and chronic transplant rejection.[13,14] Almost all research has focused on MPA and its derivatives for inhibitory immunosuppressive properties, while IMPDH is overexpressed in many types of cancer compared to normal cells. Inhibition of IMPDH can suppress the proliferation of and induce apoptosis in cancer cells.[15] Therefore, MPA and derivatives might function as anticancer agents.[16−18] Recently, rekindled interest has focused on synthesizing novel mycophenolic acid derivatives regarding their anticancer efficacy.

Typically, silicon-containing analogues are considered valuable structural moieties in pharmaceuticals and natural bioactive molecules because silicon-containing compounds are more lipophilic than their carbon counterparts.[19] For instance, karenitecin[20] and silatecan[21] are used clinically to inhibit topoisomerase I with potent anticancer activity. The organo-silicon drug cisobitan can significantly inhibit prostate cancer.[22] Silicon-containing andrographolide compounds

Received: August 14, 2024
Revised: October 5, 2024
Accepted: October 8, 2024
Published: October 17, 2024

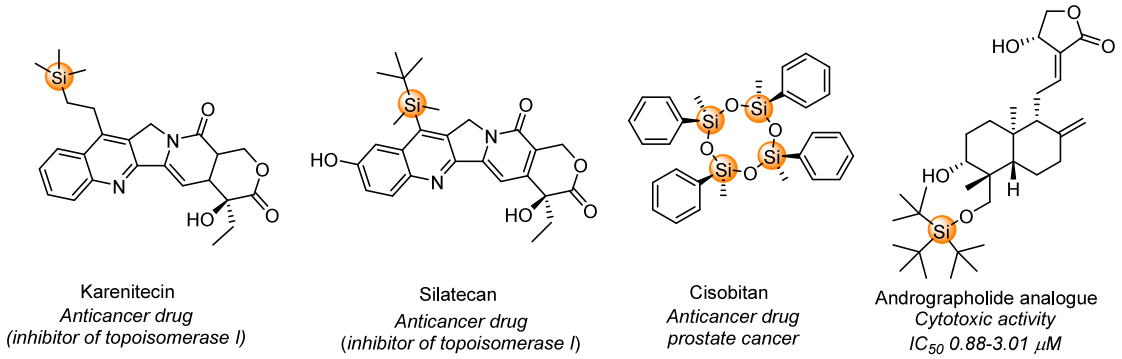

Figure 1. Biologically active silicon analogues.

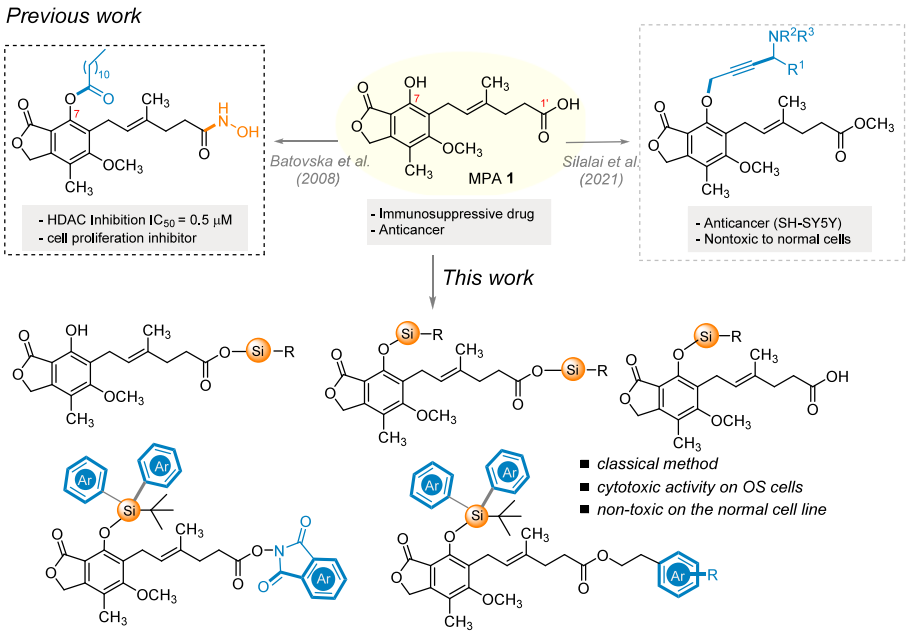

Figure 2. Mycophenolic acid (MPA) **1**, and derivatives.

Scheme 1. Synthesis of Silyl and Trityl Analogues of MPA 2 and 3[a]

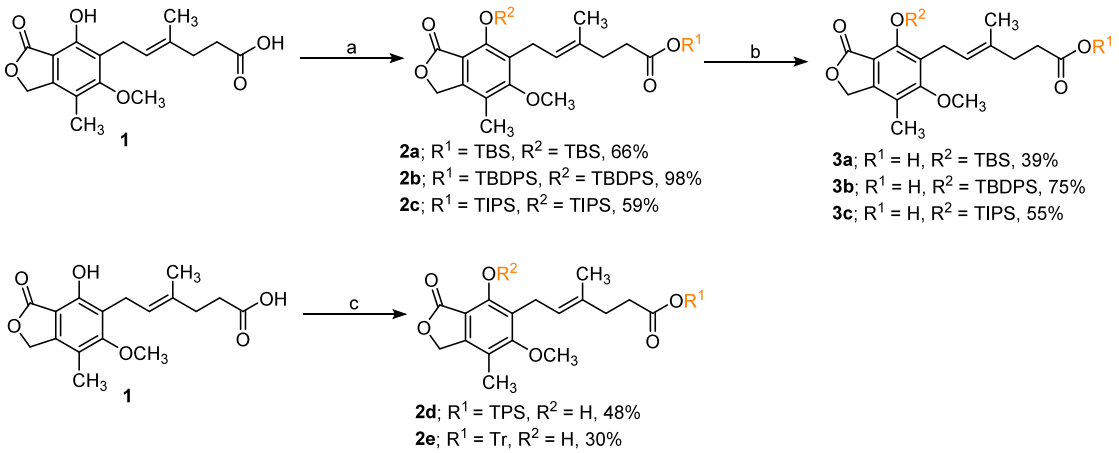

[a]Reaction conditions (a) R-Cl (8−10 equiv), imidazole (8−10 equiv) 80 °C, DMF, 24 h. (b) HCOOH:H_2O (9:1), THF, 0 °C-rt. (c) R-Cl (3.0 equiv), Et_3N (3.0 equiv), rt, DMF, 24 h, TBS = *tert*-butyldimethylsilyl, TBDPS = *tert*-butyldiphenylsilyl, TIPS = triisopropylsilyl, TPS = triphenylsilyl and Tr = triphenyl.

have shown better anticancer activity in human cancer cells than parent andrographolide (Figure 1).[23,24] Given the rich applications of anticancer activity, our design concept was built on previous reports that replacing the silicon moieties would generate new analogues with potential anticancer activity and show good lipophilicity properties.

https://doi.org/10.1021/acsbiomedchemau.4c00079
ACS Bio Med Chem Au 2025, 5, 106−118

We then focused on exploring new MPA compounds with enhanced anticancer activity. Batovska et al.[25] have synthesized a series of hydroxamic acid-MPA derivatives and studied the anticancer activity of these compounds. One of the synthesized compounds bearing lauroyloxy group at C-7 showed potent inhibitory activities against HDACs, which had been proven to exert their effective anticancer activity with an IC_{50} value of 0.5 μM. In our previous work (2021),[6] we designed a series of propargylamine mycophenolate derivatives that showed selective inhibition of neuroblastoma (SH-SY5Y) cancer cell lines and were nontoxic to normal cells. Inspired by these works, we designed and synthesized a series of mycophenolic acid derivatives by classical method silylation and esterification and evaluated all synthetic analogues for cytotoxic activity against four OS cancer cells (Figure 2).

RESULTS AND DISCUSSION

Chemistry

The preparation of silyl-MPAs **2** and **3** is outlined in Scheme 1. Silylation of MPA **1** with silyl chloride (R-Cl; R = TBS, TBDPS, TIPS) in DMF afforded derivatives **2a−2c** (R^1R^2 = TBS, TBDPS, TIPS) in 59−98% yields followed by the selective desilylation reaction of **2a−2c** (R^1R^2 = TBS, TBDPS, TIPS) with HCOOH:H_2O (9:1) in THF at 0 °C gave compounds **3a−3c** (R^1 = H, R^2 = TBS, TBDPS, TIPS) in 39−75% yields. Next, triphenylsilyl chloride (TPS) and triphenyl chloride (TrCl) were used as bulky protecting groups. MPA **1** was synthesized using Et_3N as the base in DMF, affording compounds **2d** (R^1 = TPS, R^2 = H) and **2e** (R^1 = Tr, R^2 = H) in yields of 48 and 30%, respectively.

The next series of silyl ester analogues of MPA **4** (R^1 = TBS, TBDPS, TIPS, R^2 = H) are shown (Scheme 2). The reaction carried out in pyridine and silyl chloride (R^1 = TBS, TBDPS, TIPS) gave the silyl-protected analogues **4b** (R^1 = TBDPS, R^2 = H) and **4c** (R^1 = TIPS, R^2 = H) in 66 and 55% yield, respectively while **4a** (R^1 = TBS, R^2 = H) was not stable.

Scheme 2. Synthesis of Silyl Ester Analogues of MPA 4[a]

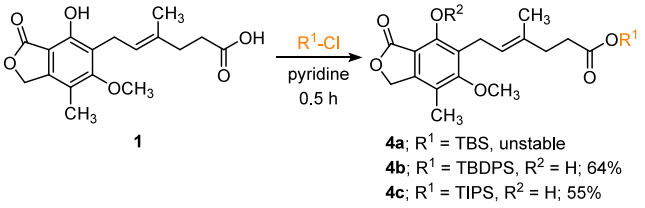

[a]Reaction conditions: MPA **1** (100 mg, 0.3121 mmol), pyridine 0.5 mL, R^1-Cl (0.4682 mmol). TBS = *tert*-butyldimethylsilyl, TBDPS = *tert*-butyldiphenylsilyl, TIPS = triisopropylsilyl.

Further, the MPA **1** was converted to the phthalimide ester analogue of MPA **6a** in low yield due to the phenol group in MPA **1** not being protected, as shown in Scheme 3.

Through this method, we can obtain the esterification products in high yield when changing the substrate. TBDPS-protected phenol of MPA **3b** (R^1 = H, R^2 = TBDPS) was utilized as a starting material for the synthesis of new mycophenolate analogues **5a−5c** by reactions with different alcohol compounds, namely, *N*-hydroxyphthalimide, 2-(4-fluorophenyl)ethanol and 2-(4-methoxyphenyl)ethanol affording **5a−5c** in 65−98% yields respectively (Scheme 4).

Scheme 4. Synthesis of Mycophenolate Analogues 5a−5c

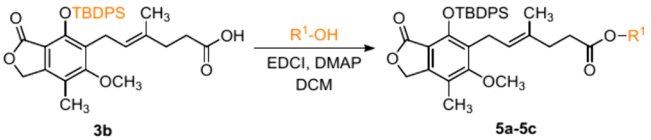

Compounds	R^1	yield (%)
5a		98
5b	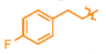	84
5c	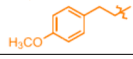	65

[a]Reaction conditions: *tert*-butyldiphenylsilyl ether-MPA product (**3b**) (0.090 mmol), DMAP (0.0090 mmol), EDCI (0.3125 mmol), R^1−OH (0.135 mmol) in DCM 1.0 mL. DMAP = 4-dimethylaminopyridine, EDCI = 1-ethyl-3-(3-(dimethylamino)propyl)carbodiimide.

For the derivatives of the unprotected phenol, desilylation of compounds **5b** and **5c** using TBAF in MeOH, furnishing **6b** and **6c** in a yield of 50 and 99% respectively (Scheme 5).

Cytotoxic Studies

Cell Viability Using MTT Assay. The cell viability and survival of the cells will be evaluated using a microculture tetrazolium (MTT) assay. MNNG/HOS, U2OS, 143B, and SaOS-2 human osteosarcoma cell lines, and human normal osteoblastic cell lines (hFOB 1.19) were obtained from the ATCC. Osteosarcoma cells at 5 × 10^3 cells will be seeded in each well of a 96-well plate and allowed to attach at 37 °C in a 5% CO_2 incubator overnight. On the following day, the cells will be treated with mycophenolic acid derivatives for 72 h. After the treatment period, culture media will be removed and replaced with 100 μL of freshly prepared 0.5 mg/mL MTT

Scheme 3. Synthesis of Phthalimide Ester of MPA 6a[a]

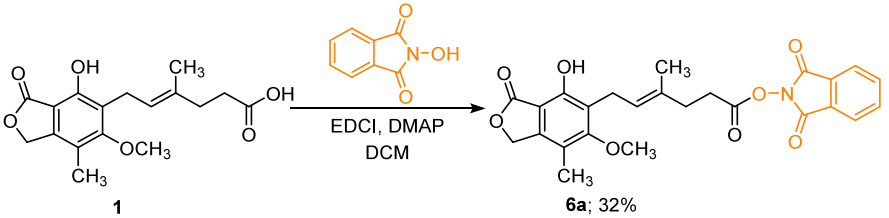

[a]Reaction conditions: MPA **1** (0.3121 mmol), DMAP 0.03125 mmol), EDCI (0.3125 mmol), *N*-hydroxyphthalimide (0.4688 mmol) in DCM 2.0 mL. DMAP = 4-dimethylaminopyridine, EDCI = 1-ethyl-3-(3-(dimethylamino)propyl)carbodiimide.

https://doi.org/10.1021/acsbiomedchemau.4c00079
ACS Bio Med Chem Au 2025, 5, 106−118

Scheme 5. Synthesis of Mycophenolic Acid Derivatives 6b and 6c[a]

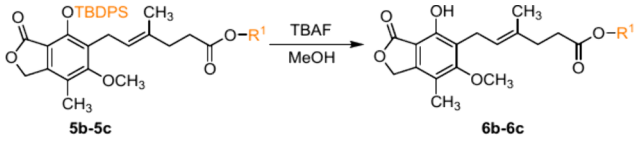

Compounds	R^1	yield (%)
6b	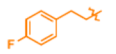	50
6c	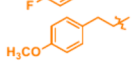	99

[a]Reaction conditions: **5b** and **5c** (50 mg), TBAF (0.02793 mmol) in MeOH 1.0 mL at 0 °C for 30 min. TBAF = tetrabutylammonium fluoride.

(A2231, AppliChem, Germany) in a culture medium and incubated at 37 °C for 2 h. After incubation, the reagent will be removed. Formazan crystals will be then dissolved in 100 μL of DMSO with agitation on a plate shaker. The optical density (OD) will be measured using a microplate reader at 570 nm wavelength. Survival rate of cell (%) = (OD of experiment group/OD of the control group) × 100%. The studies were performed in triplicate.

Measurement of IMPDH Activity in Osteosarcoma Cells. The inhibitory assay of human IMPDH1 and IMPDH2 (R&D Systems, USA) was performed by varying concentrations of the candidate IMPDH inhibitors and MPA (0.001 to 100 μM) with fixed concentrations of IMP (100 μM for IMPDH1 and 250 μM for IMPDH2) and NAD^+ (200 μM for IMPDH1 and 500 μM for IMPDH2). The assays were performed in assay buffers under the following conditions: IMPDH1; 50 mM Tris, 300 mM NaCl, pH8.0; and IMPDH2; 50 mM Tris, 300 mM NaCl, 1 mM EDTA, and 1 mM DTT, pH 8.0. First, 25 μL of varying concentrations of candidate IMPDH inhibitors and MPA were loaded into a 96-well UV plate (Greiner Bio-one, Germany) followed by 25 μL of 40 μg/mL of the rhIMPDH enzyme (1 μg). For reaction control, 25 μL of assay buffer was loaded instead of the inhibitor. For the substrate blank, 50 μL of assay buffer was loaded. The reactions were started by adding 50 μL of 2× substrate mixture (IMP and NAD^+). Kinetic analysis of IMPDH enzyme activity was performed by the measurement of NADH production at a wavelength of 340 nm every 1 min for 5 min. The enzyme velocity (μM/min) was calculated from absorbance using the molar extinction coefficient of the absorbing molecule in Beer's law equation (6220 M^{-1} cm^{-1}).

The apparent tight-binding inhibition constants ($K_{i,app}$) were calculated from enzyme velocity following Morrison's eq 2 to assess the strength of enzyme/inhibitor binding using the Dynafit program.[26−28]

$$v = v_0 \frac{[E] - [I] - K_{i,app} + \sqrt{([E] - [I] - K_{i,app})^2 + 4[E]K_{i,app}}}{2[E]} \quad (1)$$

In eq 1, v_0 is the initial velocity in the absence of the inhibitor; $[E]$ is the enzyme concentration; and $[I]$ is the inhibitor concentration.

MPA **1** and mycophenolic acid analogues **2**−**6** were screened to inhibit the growth of four osteosarcoma cell lines and the IC_{50} values were listed in Table 1. The results showed that MPA **1** exhibited cytotoxicity on all OS cell lines with IC_{50} ranging from 0.64 to 4.00 μM. Modification by silylation of MPA **1** to give silyl-protected analogues of MPA (R^1R^2 = TBS; **2a**) and (R^1R^2 = TBDPS; **2b**) displayed high activity against all OS cell lines with IC_{50} values ranging from 1.36 to 5.43 and 1.18−5.85 μM, respectively. The comparison of the results shows that the activity of (R^1R^2 = TBS; **2a**) and (R^1R^2 = TBDPS; **2b**) was better than analog (R^1R^2 = TIPS; **2c**) with a bulky group (IC_{50} 6.82−63.85 μM) in terms of in vitro cytotoxic activity against all OS cell lines (Table 1, entries 2−4). In MNNG cells, compound **2d** (R^1 = TPS, R^2 = H) with a triphenyl silyl substitution and nonsubstitution of phenol showed great cytotoxicity of 0.64 μM, which is similar to MPA **1** (0.64 μM). Another triphenyl group in compound **2e** (R^1 = Tr, R^2 = H) also displayed remarkable cytotoxicity against

Table 1. In Vitro Cytotoxicity, of MPA 1, and Derivatives 2−6

entry		cytotoxic activity IC_{50} (μM)[a]			
	compd.	143B	MNNG	U2OS	SaOS
1	MPA **1**	1.55 ± 0.49	0.64 ± 0.08	0.68 ± 0.04	4.00 ± 0.28
2	**2a**	4.12 ± 0.28	1.36 ± 0.76	3.80 ± 0.88	5.43 ± 2.87
3	**2b**	5.85 ± 0.54	1.18 ± 0.74	2.52 ± 0.96	5.80 ± 1.15
4	**2c**	63.15 ± 3.20	6.82 ± 3.51	24.43 ± 0.04	17.38 ± 9.03
5	**2d**	**1.65 ± 0.26**	**0.64 ± 0.15**	**1.01 ± 0.40**	**2.27 ± 0.68**
6	**2e**	**5.13 ± 1.10**	**0.68 ± 0.11**	**0.98 ± 0.035**	**4.83 ± 0.50**
7	**3a**	3.90 ± 0.76	**0.86 ± 0.20**	2.31 ± 1.26	4.55 ± 2.60
8	**3b**	4.74 ± 0.76	1.15 ± 0.35	2.96 ± 2.32	4.58 ± 1.05
9	**3c**	6.31 ± 0.40	2.68 ± 1.02	3.75 ± 1.06	5.44 ± 0.82
10	**4b**	6.80 ± 1.41	13.00 ± 4.24	1.85 ± 0.07	1.85 ± 0.35
11	**4c**	35.00 ± 9.90	5.70 ± 0.71	**0.92 ± 0.00**	5.50 ± 1.51
12	**5a**	31.00 ± 1.41	19.50 ± 3.54	10.25 ± 3.89	12.00 ± 0.00
13	**5b**	ND	ND	ND	ND
14	**5c**	14.50 ± 4.95	43.50 ± 2.12	10.25 ± 1.06	39.5 ± 0.71
15	**6a**	4.85 ± 1.48	ND	1.38 ± 0.60	6.90 ± 0.00
16	**6b**	2.00 ± 0.14	ND	7.00 ± 2.12	5.75 ± 1.06
17	**6c**	2.60 ± 0.28	38.00 ± 11.31	7.35 ± 1.63	9.00 ± 1.41

[a]IC_{50} values (drug concentration causing 50% growth inhibition) in μM, ND = Not determined.

https://doi.org/10.1021/acsbiomedchemau.4c00079
ACS Bio Med Chem Au 2025, 5, 106−118

MNNG (IC_{50} = 0.68 μM) and U2OS cells (0.98 μM) respectively. Compounds **2d** (R^1 = TPS, R^2 = H) and **2e** (R^1 = Tr, R^2 = H) exhibited good inhibition against all OS cell lines with IC_{50} values ranging from 0.64 to 2.27 and 0.68−5.13 μM. The triphenyl group may interact well with the target molecule, enhancing binding and biological activity. Modification of MPA **1** by introducing TBDPS and TIPS group **4b** (R^1 = TBDPS, R^2 = H) and **4c** (R^1 = TIPS, R^2 = H at R^1 position led to the appearance of cytotoxicity against U2OS with an IC_{50} value of 1.85 and 0.92 μM respectively (Table 1, entries 10 and 11). Remarkably, the free phenol of MPA derivatives **2d** (R^1 = TPS, R^2 = H), **2e** (R^1 = Tr, R^2 = H), **4b** (R^1 = TBDPS, R^2 = H) and **4c** (R^1 = TIPS, R^2 = H) with various R^1 (TPS-, Tr-, TBDPS-, TIPS-) of carboxylic acid analogues showed enhancement in cytotoxic activity. It should be noted that the inhibitory activities against all OS cell lines were somewhat positively improved by introducing the free phenol group. Meaningfully, the inhibitory activities of free carboxylic acid (**3a−3c**; R^1 = H, R^2 = TBS, TBDPS, TIPS) against all OS cell lines were relatively better than (**2a−2c**; R^1R^2 = TBS, TBDPS, TIPS), especially **3a** (R^1 = H, R^2 = TBS), which had a TBS-group substituent placed at the R^2 position shown as the most attractive molecule with an IC_{50} value of 0.86 μM in MNNG cell line. Compounds **3b** (R^1 = H, R^2 = TBDPS) and **3c** (R^1 = H, R^2 = TIPS) having a TBDPS- and TIPS- substituent at the R^2 position were found to be active against MNNK cancer cells with IC_{50} 1.15 and 2.68 μM respectively (Table 1, entries 8 and 9).

On the contrary, the esterification products **5a−5c** with TBDPS substitution at the R^2 position on the phenol resulted in lower activities with IC_{50} more than 10 μM toward all OS cancer cells. Compound **5b**, having a 4-fluorophenethylester, performed less efficiently than the rest of the phthalimide ester **5a** and 4-methoxyphenethylester **5c**. Due to the free phenol of MPA **1** being a key position in the cytotoxic activity. Attempts to enhance the cytotoxicity resulted in the removal of the TBDPS group at the R^2 position. Analogues **6a−6c** based on ester analogues **5a−5c** returned more promising levels of cytotoxicity. Compounds **6a−6c** showed IC_{50} values in the range of 1.38−9.00 μM in three OS cell lines and no cytotoxic effects on the MNNG cell line (Table 1, entries 15−17). Among the three compounds tested (**6a−6c**), phthalimide ester **6a** exhibited remarkable cytotoxicity in U2OS cell lines showing an IC_{50} of 1.38 μM and better than **5a**. Therefore, the analogues that were obtained after deprotection of R^2 at the phenol showed better activity profiles than all of the corresponding protected analogues.

Among all compounds examined for cytotoxicity in Table 1, compound **2d** (R^1 = TPS, R^2 = H) was the most potent against all four OS cancer cell lines. Silicon incorporation can be used to increase the biological activity of the target molecule.[29] Therefore, we studied the effect of silicon **2d** (R^1 = TPS, R^2 = H) and carbon **2e** (R^1 = Tr, R^2 = H) on the cytotoxic activity. In the cases of triphenyl silyl analogue **2d** (R^1 = TPS, R^2 = H) was approximately 2 to 3-fold more potent than its corresponding carbon compound **2e** (R^1 = Tr, R^2 = H) by inhibiting two specific OS cancer cell lines (143B and SaOS). Also, the lactone function, phenol, and triphenyl group in compound **2d** (R^1 = TPS, R^2 = H) can engage in various interactions with biomolecular targets, including hydrogen bonding, $\pi-\pi$ stacking, and dipole interactions (Figure 3). The study suggests that the incorporation of silicon (Si) into structure **2d** (R^1 = TPS, R^2 = H) led to an increase in its cytotoxic activity.

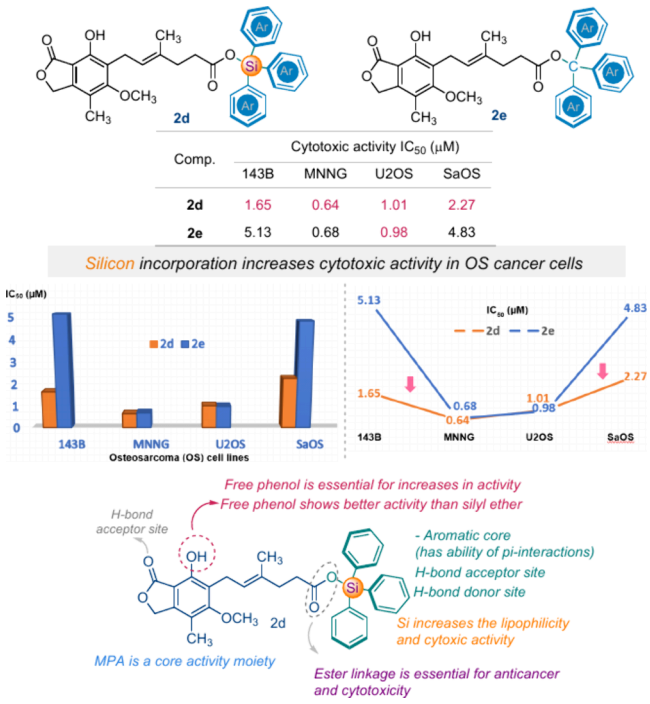

Figure 3. Most active compound of MPA derivative **2d**.

Regarding the safety of **2d** (R^1 = TPS, R^2 = H) toward the normal cell line, compound **2d** (R^1 = TPS, R^2 = H) showed low cytotoxicity to human normal osteoblast cells (hFOB 1.19) at the tested concentrations, introducing that this compound is much less cytotoxic to normal cells as compared to OS cancer cells (Table 2). Therefore, compound **2d** (R^1 = TPS, R^2 = H) led to significant development in cytotoxicity against the OS cancer cell line and nontoxic on the normal cell line (hFOB 1.19) compared with MPA **1**.

Inosine monophosphate dehydrogenase 2 (IMPDH2) is an enzyme that plays an important role in the biosynthesis of guanine nucleotides, which are essential for DNA and RNA synthesis, and related to cell differentiation, tumor transformation, and rapidly increasing tumor cells.[30,31] Cancer cells often require elevated levels of nucleotides to support their uncontrolled growth and division.[31,32] In some cases, overexpression or increased activity of IMPDH2 has been observed in cancers such as the fatal brain tumor glioblastoma, acute myelogenous leukemia (AML), and chronic myelogenous leukemia (CML).[33,34] From these results, it might be possible to cure some cancers by blocking the IMPDH-mediated de novo pathway of guanine nucleotide production.[35] Therefore, a renewed determination is being made on the anticancer potential of IMPDH inhibitors. MPA **1** is an inhibitor of IMPDH and is a known anticancer and immunosuppressive agent. Table 3 illustrates that MPA **1** has promising activity against both IMPDH 1 and IMPDH 2 enzymes with $K_{i,app}$ values of 0.136 and 0.046 μM, respectively. In our study, MPA **1** was further modified to explore new and selective inhibitors of IMPDH2. However, we found that compound **2d** (R^1 = TPS, R^2 = H) did not exhibit potent inhibition of either IMPDH1 or IMPDH2 compared to that of MPA **1**.

https://doi.org/10.1021/acsbiomedchemau.4c00079
ACS Bio Med Chem Au 2025, 5, 106−118

Table 2. Cytotoxic Effect of Mycophenolic Acid Analogues in Osteoblast Cell Lines hFOB 1.19

	cell viability of hFOB 1.19[a] ± SD (%)			
compounds	0.1 μM	1.0 μM	10.0 μM	100.0 μM
control	100			
MPA **1**	74.3 ± 4.24	20.14 ± 1.41	7.13 ± 0.67	3.38 ± 3.40
2d	93.91 ± 1.01	91.95 ± 1.78	84.5 ± 2.95	73.34 ± 1.39

[a]Cell viability (%): the cell viability in control was taken as 100%, all data were expressed as mean ± SD (n = 3). hFOB 1.19 = human fetal osteoblastic cell line.

Table 3. Selected Inhibitors of IMPDH

	$K_{i,app}$ (μM)[a]	
compounds	IMPDH1	IMPDH2
MPA **1**	0.136	0.046
2d	NO	1.8

[a]The apparent tight-binding inhibition constants ($K_{i,app}$) in μM, NO = No inhibition observed.

Computational Docking

Molecular docking calculations for model compounds were employed to illustrate the factors resolving the cytotoxic activity of the studied MPA derivatives. MPA analogues were explored for the first time on cytotoxicity to osteosarcoma cancer cells, confirming the important role played by the molecular docking method in understanding the interaction mode of MPA derivatives.

Vascular endothelial growth factor (VEGF) is a highly specific vascular endothelial growth factor overexpressed in tumor cells which release higher levels of VEGF compared to normal cells.[36,37] The VEGFR-2 subtype is the most critical regulator of the angiogenesis process and plays an important role in the dissolution, migration, and proliferation of endothelial cancer cells. Targeting VEGFR-2 specifically can be an effective way to inhibit the angiogenic process in osteosarcoma and potentially slow down tumor growth and metastasis.[38] Therefore, the anti-VEGFR-2 subtype is an essential form of suppressing OS tumor growth and metastasis.

Molecular docking was employed to explain the promising VEGFR-2 inhibitory activity of the mycophenolic acid analogues by finding their binding mode and their interaction with the critical amino acids (Glu885, Cys919, and Asp1046) in the active site of the VEGFR-2. In our work, we selected (PDB ID: 4ASD) as the protein data bank for VEGFR-2 to screen three compounds (MPA **1**, **2d**, and **5c**) in molecular docking studies.[39]

MPA **1** displayed the binding energy values of −6.60 kcal/mol with VEGFR-2 and was involved in strong hydrogen bonding with the key amino acids Cys919 and Asp1046 via the carbonyl of lactone, phenol, and carboxylic acid at a distance of 2.05, 2.24, and 1.78 Å respectively because these three functional groups highly boosted cytotoxic efficiency (Figure 4). Compound **2d** (R^1 = TPS, R^2 = H) exhibits the best experimental cytotoxic activity against all four OS cancer cell lines with IC_{50} ranging from 0.64 to 2.27 μM and showed the highest predicted binding affinity with a docking score of−9.11 kcal/mol. Also, the hybridization of the triphenyl silyl group with the MPA scaffold **2d** (R^1 = TPS, R^2 = H) binds in the same favorable hydrogen bond and with the backbone of Asp1046 via the oxygen atom of phenol (distance: 2.05 Å) as shown in Figure 5. The triphenyl silyl substitution of carboxylic acid increases the hydrophobic interaction with the key amino

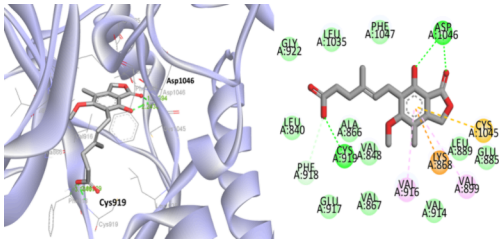

Figure 4. Proposed binding mode of MPA **1** in the active site of VEGFR-2 (PDB code: 4ASD).

acid Glu885 and Asp1046 enhancing the binding interaction, as can be shown in its docking score (−9.11 kcal/mol) when compared to the MPA **1** (−6.60 kcal/mol) (Table 4). Due to the low cytotoxic activity of all four OS cancer cell lines in this series, compound **5c** was selected to study molecular docking interactions in the active site of VEGFR-2. Docking results of compound **5c** showed poor binding affinity and did not bind at the key amino acids of the active site which may be because of steric clashes with the VEGFR-2 binding site (Table 4). Accordingly, the obtained results confirmed that the molecular docking was consistent with the cytotoxic activities of the tested compounds.

The cyclin-dependent kinases (CDKs) play an essential role in cell cycle progression and are validated as cancer therapy targets. CDK2 is commonly overexpressed in human tumors and is necessary for the proliferation of tumor cells.[40,41] Although rare, osteosarcoma is an aggressive cancer that often metastasizes to other organs. In addition, the research studies evidenced that the cyclin-dependent kinase (CDK) inhibitor proved to induce the apoptosis of several osteosarcoma cell lines.[42] The molecular docking study was employed to understand the binding of the most potent compound **2d** (R^1 = TPS, R^2 = H) from the Protein Data Bank with PDB code 2a4l to study their interactions with the key amino acids in the active site of the CDK2 enzyme to explain the structure−activity relationship (SARs) (Table 5).[43]

As shown in the docking mode of compound **2d** (R^1 = TPS, R^2 = H) with CDK2, the phenol and ester of **2d** (R^1 = TPS, R^2 = H) have the potential to form two hydrogen bonds with the essential Leu83 and Lys89 residues. Moreover, the triphenylsilyl group and aromatic phenol are extended in the pocket to form a hydrophobic interaction with the surrounding Asp86 and His84 amino acids (Figure 6). To better understand the SARs study shows that the free phenol group attached to MPA can form favorable interactions in the active site of CDK2.

To provide a basis for identifying IMPDH inhibitors as anticancer agents, molecular docking was conducted to show the potential binding mode of compound **2d** (R^1 = TPS, R^2 = H) with the IMPDH enzymes (PDB: 1JR1).[44,45] This compound could interact with the key amino acid residues in the active site of the enzyme, including hydrogen-bonding

https://doi.org/10.1021/acsbiomedchemau.4c00079
ACS Bio Med Chem Au 2025, 5, 106−118

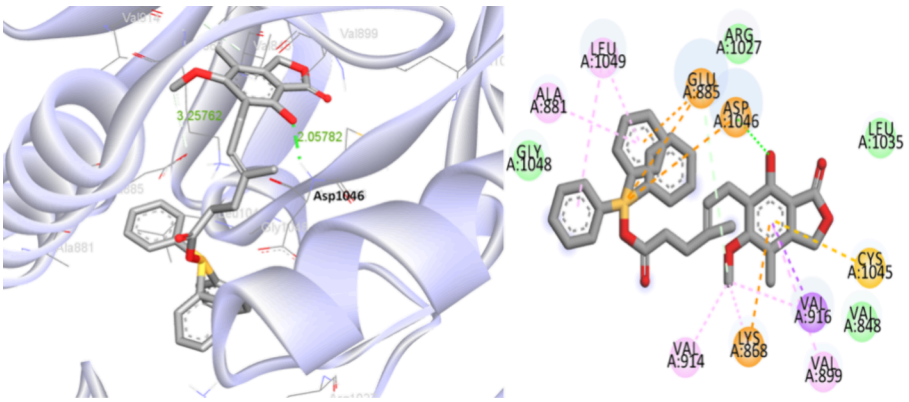

Figure 5. Proposed binding mode of compound **2d** in the active site of VEGFR-2 (PDB code: 4ASD).

Table 4. Molecular Docking Analysis of VEGFR-2 with MPA 1 and Mycophenolic Acid Analogues 2d and 5c[a]

		intermolecular hydrogen bonding			
compounds	binding energy (kcal/mol)	amino acids interaction	distance (Å)	interaction groups	intermolecular hydrophobic contacts
MPA **1**	−6.60	Asp1046	1.78	CO of lactone	Val916, Lys868, Val899, Cys1045
		Asp1046	2.24	OH of phenol	
		Cys919	2.05	OH of COOH	
2d	−9.11	Asp1046	2.05	OH of phenol	Asp1046, Ala881, Glu885, Leu1049, Cys1045, Lys868, Val916
5c	−6.81				Asp1046, Leu1049, Arg1027, Val898, Leu1019

[a]The binding energies were evaluated using AutoDock.

Table 5. Molecular Docking Analysis of CDK2 with Mycophenolic Acid Analogue 2d[a]

		intermolecular hydrogen bonding			
compounds	binding energy (kcal/mol)	amino acids interaction	distance (Å)	interaction groups	intermolecular hydrophobic contacts
2d	−8.63	Leu83	2.15	OH of phenol	Val18, Leu134, Asp86
		Lys89	1.84	CO of ester	

[a]The binding energies were evaluated using AutoDock.

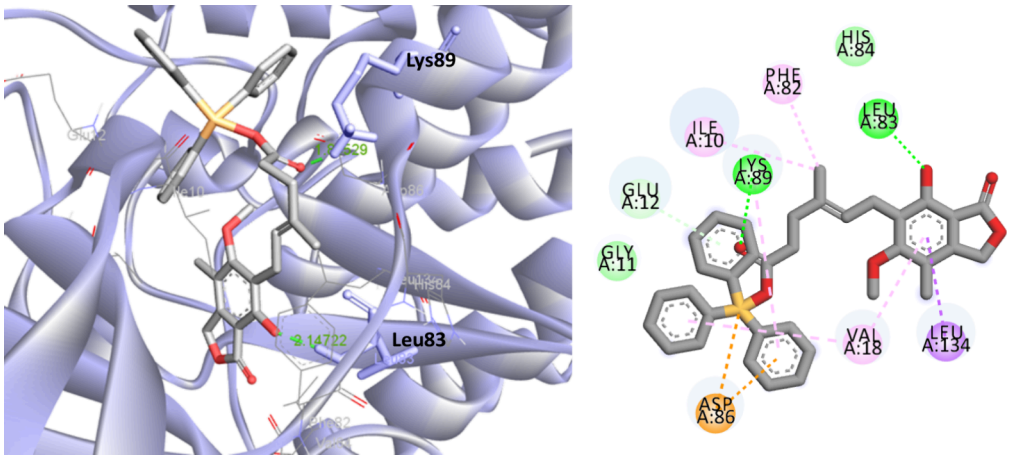

Figure 6. Proposed binding mode of compound **2d** in the active site of CDK2 (PDB code: 2a4l).

interactions between the carbonyl group of the lactone ring and THR333. Similarly, the phenol group on the compound **2d** (R^1 = TPS, R^2 = H), as a hydrogen donor, also interacted with THR333. The oxygen atom of lactone forms a hydrogen bonding interaction with the backbone NH moiety of GLY326 that is necessary for efficient inhibitors. At the same time, the carbonyl group of ester ($COOSiPh_3$) forms a hydrogen bonding interaction with Ser276 (Table 6 and Figure 7).

CONCLUSIONS

In this work, a new series of mycophenolic acid analogues **2**−**6** were synthesized by using convenient reactions to enhance the cytotoxic activity of MPA. All synthetic analogues were tested for cytotoxicity against four OS cancer cell lines. The triphenyl silyl analog **2d** (R^1 = TPS, R^2 = H) showed potent cytotoxicity and selectivity to OS cancer cells than MPA **1** and displayed

https://doi.org/10.1021/acsbiomedchemau.4c00079
ACS Bio Med Chem Au 2025, 5, 106−118

Table 6. Molecular Docking Analysis of IMPDH with Mycophenolic Acid Analogue 2d[a]

		intermolecular hydrogen bonding			
compounds	binding energy (kcal/mol)	amino acids interaction	distance (Å)	interaction groups	intermolecular hydrophobic contacts
2d	−8.02	THR333	2.62	OH of phenol	SER275, PHE282
		THR333	2.01	CO of lactone	
		GLY326	2.09	O of lactone	
		SER276	1.75	CO of ester	

[a]The binding energies were evaluated using AutoDock.

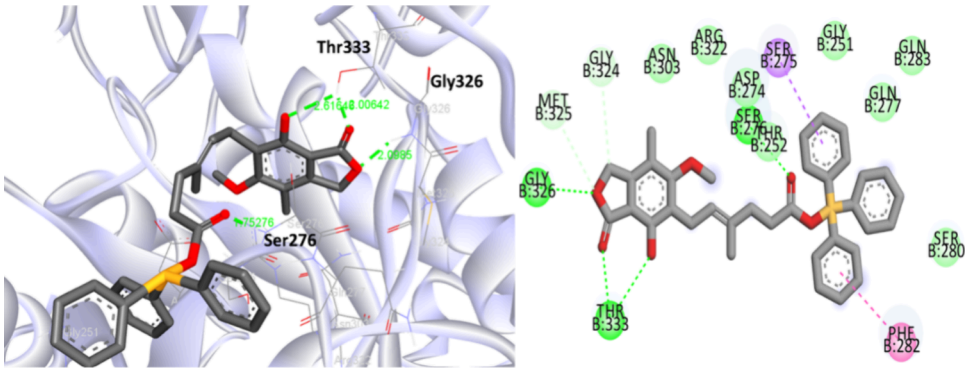

Figure 7. Proposed binding mode of compound **2d** in the active site of IMPDH (PDB code: 1JR1).

the strongest IC_{50} values ranging from 0.64 to 2.27. The triphenyl analogue **2e** (R^1 = Tr, R^2 = H) also showed high cytotoxicity (IC_{50} = 0.68−5.13 μM). The triphenyl group and free phenol group in MPA play a significant impact on cytotoxicity. The molecular docking represents the poses of triphenyl silyl-MPA **2d** (R^1 = TPS, R^2 = H) on three cancer proteins (VEGFR-2, CDK2, and IMPDH). Computational studies revealed that compound **2d** (R^1 = TPS, R^2 = H) possesses a high affinity for VEGFR-2 (−9.11 kcal/mol), CDK2 (−8.63 kcal/mol), and IMPDH (−8.02 kcal/mol). Our results showed the triphenyl silyl of MPA plays a very significant role in cytotoxic activity against cancer cell lines. Our synthetic MPA analogues might serve as a starting point of building blocks for future structure modification against OS cancer cells.

EXPERIMENTAL SECTION

General Information

All chemicals and mycophenolic acid as a starting material (CAS NO. 24280-93-1) were purchased from commercial sources and used without further purification. Proton NMR spectra were recorded by using a BRUKER AVANC (400 MHz) spectrometer. All spectra were recorded in the $CDCl_3$ solvent, chemical shifts are reported as δ values in parts per million (ppm) relative to tetramethylsilane (δ 0.00), and $CDCl_3$ (δ 7.26) was used as an internal standard. Carbon NMR spectra were recorded on a BRUKER AVANC (100 MHz) spectrometer. All spectra were recorded in $CDCl_3$ solvent and chemical shifts are reported as δ values in parts per million (ppm) relative to $CDCl_3$ (δ 77.0) as an internal standard. High-resolution mass spectrometry (HRMS) data were recorded at Naresuan University. Analytical thin-layer chromatography (TLC) was conducted on precoated TLC plates; silica gel 60F-254 [E. Merck, Darmstadt, Germany]. Silica gel columns for open-column chromatography utilized silica gel 60 PF254 [E. Merck, Darmstadt, Germany]. Melting points were measured using a melting point apparatus (Griffin) and are uncorrected.

General Procedure for the Preparation of Silyl Ether-MPA Analogues (2a−2c)

MPA **1** (100 mg, 0.3121 mmol), silyl chloride (R-Cl; R = TBS, TBDPS, TIPS) (1.8726 mmol), and imidazole (170 mg, 2.4968 mmol) were dissolved in dry DMF (2 mL), and the reaction mixture was stirred at room temperature for 24 h. After TLC showed the reaction completed, the mixture was quenched with saturated NH_4Cl solution, then extracted with EtOAc, and washed with brine. The combined organic layers were dried over anhydrous Na_2SO_4 and the solvent was removed by rotary evaporation. The crude product was purified by column chromatography.

Synthesis of *tert*-Butyldimethylsilyl (*E*)-6-(4-((*tert*-Butyldimethylsilyl)oxy)-6-methoxy-7-methyl-3-oxo-1,3-dihydroisobenzofuran-5-yl)-4-methylhex-4-enoate (2a). MPA **1** (100 mg, 0.3121 mmol), *tert*-butyldimethylsilyl chloride (282 mg, 1.8726 mmol), and imidazole (170 mg, 2.4968 mmol) were dissolved in dry DMF (2 mL), and the reaction mixture was stirred at room temperature for 24 h. The crude product **2a** was purified by column chromatography (6:1 *n*-hexane:EtOAc) to afford compound **2a** (112.5 mg) as a white solid in 66% yield.

2a: A white solid in 66% yield; Mp: 76.6−80.6 °C; R_f = 0.79 (2:1 *n*-hexane:EtOAc); ^{1}H NMR (400 MHz, $CDCl_3$): δ 5.18 (1H, t, J = 6.4 Hz), 5.05 (2H, brs), 3.73 (3H, s), 3.37 (2H, d, J = 6.4 Hz), 2.40−2.33 (2H, m), 2.30−2.22 (2H, m), 2.14 (3H, s), 1.75 (3H, s), 1.02 (9H, s), 0.88 (9H, s), 0.23 (6H, s), 0.18 (6H, s); ^{13}C NMR (100 MHz, $CDCl_3$): δ 173.8, 169.2, 163.2, 151.4, 146.0, 135.2, 133.8, 127.7, 125.0, 123.3, 117.9, 111.6, 67.6, 60.7, 34.7, 34.6, 32.2, 26.4, 26.0, 25.6, 25.5, 23.6, 23.4, 18.7, 17.5, 16.4, 11.4, −3.6, −4.9 ppm; HRMS (m/z): calcd for $C_{29}H_{48}O_6Si_2Na$ $[M + Na]^+$ 571.2887, found: 571.2886.

Synthesis of *tert*-Butyldiphenylsilyl (*E*)-6-(4-((*tert*-Butyldiphenylsilyl)oxy)-6-methoxy-7-methyl-3-oxo-1,3-dihydroisobenzofuran-5-yl)-4-methylhex-4-enoate (2b). MPA **1** (100 mg, 0.3121 mmol), *tert*-butyldiphenylsilyl chloride (481 μL, 1.8726 mmol), and imidazole (170 mg, 2.4968 mmol) were dissolved in dry DMF (2 mL), and the reaction mixture was stirred at room temperature for 24 h. The crude product **2b** was purified by column chromatography (6:1 *n*-hexane:EtOAc) to afford compound **2b** (245 mg) as a white oil in 98% yield.

2b: A white oil in 98% yield; R_f = 0.74 (2:1 *n*-hexane:EtOAc); ^{1}H NMR (400 MHz, $CDCl_3$): δ 7.69 (4H, d, J = 6.8 Hz), 7.64 (4H, d, J = 6.8 Hz), 7.50−7.28 (12H, m), 5.10−4.95 (3H, m), 3.59 (3H, s), 3.16

https://doi.org/10.1021/acsbiomedchemau.4c00079
ACS Bio Med Chem Au 2025, 5, 106−118

(2H, d, J = 5.6 Hz), 2.50−2.40 (2H, m), 2.23 (2H, t, J = 8.4 Hz), 2.11 (3H, s), 1.48 (3H, s), 1.09 (9H, s), 1.07 (9H, s) ppm; ^{13}C NMR (100 MHz, $CDCl_3$): δ 172.4, 168.3, 163.1, 151.5, 145.9, 135.2, 134.9, 134.7, 133.6, 133.5, 131.8, 129.9, 129.4, 129.3, 127.6, 127.2, 123.4, 117.8, 111.1, 67.3, 60.5, 34.6, 34.3, 26.8, 26.4, 24.2, 20.3, 19.0, 16.2, 11.2 ppm; HRMS (m/z): calcd for $C_{49}H_{56}O_6Si_2Na$ [M + Na]$^+$ 819.3513, found: 819.3513.

Synthesis of Triisopropylsilyl (*E*)-6-(6-Methoxy-7-methyl-3-oxo-4-((triisopropylsilyl)oxy)-1,3-dihydroisobenzofuran-5-yl)-4-methylhex-4-enoate (2c). MPA **1** (100 mg, 0.3121 mmol), triisopropylsilyl chloride (400 μL, 1.8726 mmol), and imidazole (170 mg, 2.4968 mmol) were dissolved in dry DMF (2 mL), and the reaction mixture was stirred at room temperature for 24 h. The crude product **2c** was purified by column chromatography (5:1 *n*-hexane:EtOAc) to afford compound **2c** (117.4 mg) as a white solid in 59% yield.

2c: A white solid in 59% yield; Mp: 54−58 °C; R_f = 0.68 (2:1 *n*-hexane:EtOAc); ^{1}H NMR (400 MHz, $CDCl_3$): δ 5.16 (1H, t, J = 4.8 Hz), 5.06 (2H, s), 3.72 (3H, s), 3.39 (2H, d, J = 6.0 Hz), 2.43−2.38 (2H, m), 2.37−2.26 (2H, m), 2.14 (3H, s), 1.77 (3H, s), 1.56−1.48 (3H, m), 1.27−1.20 (3H, m), 1.24−1.00 (36H, m) ppm; ^{13}C NMR (100 MHz, $CDCl_3$): δ173.3, 169.4, 163.1, 152.7, 145.8, 133.8, 127.3, 123.7, 117.3, 111.0, 67.6, 60.6, 34.5, 23.6, 18.0, 17.6, 16.4, 14.3, 11.3, 11.0 ppm; HRMS (m/z): calcd for $C_{35}H_{60}O_6Si_2Na$ [M + Na]$^+$ 655.3826, found 655.3826.

General Procedure for the Preparation of Triphenyl Ether-MPA Analogues (2d−2e)

MPA **1** (200 mg, 0.6240 mmol), R-Cl (R = Tr, TPS) (1.872 mmol), and Et_3N (263 μL, 1.872 mmol) were dissolved in dry DMF (2 mL), and the reaction mixture was stirred at room temperature for 24 h. After TLC showed the reaction was completed, the mixture was quenched with saturated NH_4Cl solution, then extracted with EtOAc, and washed with brine. The combined organic layers were dried over anhydrous Na_2SO_4 and the solvent was removed by rotary evaporation. The crude product was purified by column chromatography.

Synthesis of Triphenylsilyl (*E*)-6-(4-Hydroxy-6-methoxy-7-methyl-3-oxo-1,3-dihydroisobenzofuran-5-yl)-4-methylhex-4-enoate (2d). MPA **1** (200 mg, 0.6240 mmol), triphenylsilyl chloride (552 mg, 1.872 mmol), and Et_3N (263 μL, 1.872 mmol) were dissolved in dry DMF (2 mL), and the reaction mixture was stirred at room temperature for 24 h. The crude product **2e** was purified by column chromatography (3:1 *n*-hexane:EtOAc) to afford compound **2e** (175 mg) as a white solid in 48% yield.

2d: A white solid in 48% yield; Mp: 114−120 °C; R_f = 0.53 (1:1 *n*-hexane:EtOAc); ^{1}H NMR (400 MHz, $CDCl_3$): δ 7.61 (6H, d, J = 6.8 Hz), 7.42−7.37 (4H, m), 7.33 (2H, s), 7.31 (3H, s), 7.28 (1H, s), 4.98 (1H, t, J = 5.2 Hz), 4.87 (2H, s), 3.67 (3H, s), 3.17 (2H, d, J = 6.0 Hz), 2.31 (2H, t, J = 7.2 Hz), 2.17 (2H, t, J = 8.4 Hz), 2.09 (3H, s), 1.54 (3H, s) ppm; ^{13}C NMR (100 MHz, $CDCl_3$): δ178.6, 168.4, 162.9, 151.2, 145.4, 135.7, 134.9, 133.5, 133.2, 130.0, 129.9, 127.8, 127.7, 127.4, 123.7, 118.3, 111.8, 67.4, 60.7, 33.9, 32.5, 23.7, 16.1, 11.3 ppm; HRMS (m/z): calcd for $C_{35}H_{34}O_6SiNa$ [M + Na]$^+$ 601.2022, found: 601.2022.

Synthesis of Trityl (*E*)-6-(4-Hydroxy-6-methoxy-7-methyl-3-oxo-1,3-dihydroisobenzofuran-5-yl)-4-methylhex-4-enoate (2e). MPA **1** (200 mg, 0.6240 mmol), trityl chloride (528 mg, 1.872 mmol), and Et_3N (263 μL, 1.872 mmol) were dissolved in dry DMF (2 mL), and the reaction mixture was stirred at room temperature for 24 h. The crude product **2d** was purified by column chromatography (5:1 *n*-hexane:EtOAc) to afford compound **2d** (103 mg) as a white solid in 30% yield.

2e: A white solid in 30% yield; Mp: 92−98 °C; R_f = 0.15 (5:1 *n*-hexane:EtOAc) ^{1}H NMR (400 MHz, $CDCl_3$): δ 7.59 (1H, s), 7.28−7.23 (6H, m), 7.23−7.12 (9H, m), 5.20 (1H, t, J = 6.8 Hz), 5.12 (2H, s), 3.65 (3H, s), 3.31 (2H, d, J = 6.8 Hz), 2.43−2.38 (2H, m), 2.24 (2H, t, J = 8.0 Hz), 2.06 (3H, s), 1.72 (3H, s) ppm; ^{13}C NMR (100 MHz, $CDCl_3$): δ172.9, 171.0, 163.7, 153.7, 146.9, 144.1, 143.4, 134.3, 128.4, 128.0, 128.0, 127.9, 127.7, 127.3, 127.2, 122.6, 116.8, 106.4, 89.8, 82.0, 70.1, 61.0, 34.3, 22.6, 16.3, 11.6 ppm; HRMS (m/z): calcd for $C_{36}H_{34}O_6Na$ [M + Na]$^+$ 585.2253, found: 585.2252.

General Procedure for the Preparation of Silyl Ether-MPA Analogues (3a−3c)

MPA **1**, silyl chloride (R-Cl; R = TBS, TBDPS, TIPS) (10 equiv), and imidazole (10 equiv) were dissolved in dry DMF (5 mL), and the reaction mixture was stirred at rt-80 °C for 24 h. After TLC showed that the reaction was completed, the mixture was quenched with saturated NH_4Cl solution. Then, extracted with EtOAc and washed with brine, the combined organic layers were dried over anhydrous Na_2SO_4, and the solvent was removed by a rotary evaporator. The crude product **2** was dissolved in THF (5 mL) and then was added HCOOH:H_2O (9:1) (5 mL) at 0 °C to the mixture and allowed to stir at room temperature for a further 2 h. After TLC indicated that the reaction was complete, the reaction mixture was diluted with EtOAc (10 mL) and quenched with cold saturated $NaHCO_3$, extracted with EtOAc and washed with brine, then dried over with Na_2SO_4 anhydrous, and concentrated *in vacuo* to obtain crude product **3**. The crude product was purified by column chromatography (*n*-hexane:EtOAc).

Synthesis of (*E*)-6-(4-((*tert*-Butyldimethylsilyl)oxy)-6-methoxy-7-methyl-3-oxo-1,3-dihydroisobenzofuran-5-yl)-4-methylhex-4-enoic acid (3a). MPA **1** (100 mg, 0.3121 mmol), *tert*-butyldimethylsilyl chloride (470 mg, 3.121 mmol), imidazole (212 mg, 3.121 mmol) were dissolved in dry DMF (5 mL), and the reaction mixture was stirred at 80 °C for 24 h to obtain crude product **2a**. The crude product was dissolved in THF (5 mL) and then was added HCOOH:H_2O (9:1) (5 mL) at 0 °C to the mixture and allowed to stir at room temperature for a further 2 h. The crude product was purified by column chromatography (3:1 *n*-hexane:EtOAc) to afford compound **3a** (52.9 mg) as a white solid in 39% yield in two steps.

3a: A white solid in 39% yield; Mp: 122−124 °C, R_f = 0.61 (1:1 *n*-hexane:EtOAc); ^{1}H NMR (400 MHz, $CDCl_3$): δ 7.29 (1H, s), 5.20 (1H, t, J = 5.6 Hz), 5.07 (2H, s), 3.74 (3H, s), 3.38 (2H, d, J = 6.0 Hz), 2.41 (2H, t, J = 6.4 Hz), 2.30 (2H, t, J = 7.6 Hz), 2.15 (3H, s), 1.76 (3H, s), 1.02 (9H, s), 0.23 (6H, s) ppm; ^{13}C NMR (100 MHz, $CDCl_3$): δ 179.2, 169.2, 163.2, 151.7, 146.1, 138.4, 127.6, 123.9, 117.9, 111.6, 67.7, 60.7, 34.1, 32.7, 26.0, 23.7, 18.7, 16.3, 11.4, −3.6 ppm; HRMS (m/z): calcd for $C_{23}H_{34}O_6SiNa$ [M + Na]$^+$ 457.2022, found: 457.2019.

Synthesis of (*E*)-6-(4-((*tert*-Butyldimethylsilyl)oxy)-6-methoxy-7-methyl-3-oxo-1,3-dihydroisobenzofuran-5-yl)-4-methylhex-4-enoic acid (3b). MPA **1** (500 mg, 1.5625 mmol), *tert*-butyldiphenylsilyl chloride (2.4 mL, 9.375 mmol), and imidazole (638 mg, 9.375 mmol) were dissolved in dry DMF (10 mL), and the reaction mixture was stirred at room temperature for 24 h to obtain crude product **2b**. The crude product was dissolved in THF (10 mL) and then HCOOH:H_2O (9:1) (10 mL) at 0 °C was added to the mixture and allowed to stir at room temperature for a further 2 h. The crude product was purified by column chromatography (3:1 *n*-hexane:EtOAc) to afford compound **3b** (0.6573 g) as a sticky white oil in 75% yield in two steps.

3b: A yellow oil in 75% yield; R_f = 0.34 (2:1 *n*-hexane:EtOAc); ^{1}H NMR (400 MHz, $CDCl_3$): δ 7.68 (4H, d J = 6.8 Hz), 7.40−7.28 (6H, m), 5.00−4.92 (4H, m), 3.60 (3H, s), 3.15 (2H, d, J = 5.6 Hz), 2.27 (2H, t, J = 7.2 Hz), 2.15 (2H, t, J = 8.4 Hz), 2.10 (3H, s), 1.46 (3H, s), 1.08 (9H, s) ppm; ^{13}C NMR (100 MHz, $CDCl_3$): δ 178.6, 168.4, 163.1, 151.5, 145.9, 134.9, 133.7, 129.4, 127.3, 123.5, 117.8, 111.2, 67.4, 60.5, 34.3, 29.6, 26.4, 24.2, 20.3, 16.0, 11.2 ppm; HRMS (m/z): calcd for $C_{33}H_{38}O_6SiNa$ [M + Na]$^+$ 581.2335, found: 581.2335.

Synthesis of (*E*)-6-(6-Methoxy-7-methyl-3-oxo-4-((triisopropylsilyl)oxy)-1,3-dihydroisobenzofuran-5-yl)-4-methylhex-4-enoic acid (3c). MPA **1** (100 mg, 0.3121 mmol), triisopropylsilyl chloride (668 μL, 3.121 mmol), and imidazole (209 mg, 3.121 mmol) were dissolved in dry DMF (5 mL), and the reaction mixture was stirred at 80 °C for 24 h to obtain crude product **2c**. The crude product was dissolved in THF (5 mL) and then was added HCOOH:H_2O (9:1) (5 mL) at 0 °C to the mixture and allowed to stir at room temperature for a further 6 h. The crude

https://doi.org/10.1021/acsbiomedchemau.4c00079
ACS Bio Med Chem Au 2025, 5, 106−118

product was purified by column chromatography (3:1 *n*-hexane:EtOAc) to afford compound **3c** (82.3 mg) as a white solid in 55% yield in two steps.

3c: A yellow solid in 55% yield; Mp: 110−114 °C, R_f = 0.24 (3:1 *n*-hexane:EtOAc); ^{1}H NMR (400 MHz, $CDCl_3$): δ 7.27 (1H, s), 5.16 (1H, t, J = 6.0 Hz), 5.06 (2H, s), 3.72 (3H, s), 3.38 (2H, d, J = 6.0 Hz), 2.41 (2H, t, J = 7.2 Hz), 2.31 (2H, t, J = 7.6 Hz), 2.13 (3H, s), 1.77 (3H, s), 1.60−1.40 (3H, m), 1.09 (18H, s) ppm; ^{13}C NMR (100 MHz, $CDCl_3$): δ 179.4, 169.5, 163.2, 152.7, 146.0, 133.4, 127.3, 124.4, 117.4, 111.1, 67.7, 60.7, 34.1, 32.7, 23.7, 18.1, 16.3, 14.3, 11.4 ppm; HRMS (m/z): calcd for $C_{26}H_{40}O_6SiNa$ $[M + Na]^+$ 499.2492, found: 499.2486.

General Procedure for the Preparation of Silyl Ether-MPA Analogues (4a−4c)

To a rapidly stirring solution of MPA, **1** (100 mg, 0.3121 mmol) in 0.5 mL of pyridine was added silyl chloride (R-Cl; R = TBS, TBDPS, TIPS) (0.4682 mmol). The reaction mixture was stirred at room temperature for 0.5 h. After TLC showed the reaction completed, the mixture was diluted with EtOAc 5 mL, quenched with saturated NH_4Cl solution, and then extracted with EtOAc. The mixture was quenched with $CuSO_4{\cdot}5H_2O$ to remove the pyridine, extracted with EtOAc, and washed with brine. The combined organic layers were dried over anhydrous Na_2SO_4, and the solvent was removed by rotary evaporation and purified by column chromatography.

Synthesis of *tert*-Butyldiphenylsilyl (*E*)-6-(4-Hydroxy-6-methoxy-7-methyl-3-oxo-1,3-dihydroisobenzofuran-5-yl)-4-methylhex-4-enoate (4b). To a rapidly stirring solution of MPA **1** (100 mg, 0.3121 mmol) in 0.5 mL of pyridine was added *tert*-butyldiphenylsilyl chloride (120 μL, 0.4682 mmol). The reaction mixture was stirred at room temperature for 0.5 h. The crude product was purified by column chromatography (5:1 *n*-hexane:EtOAc) to afford compound **4b** (112.5 mg) as a white solid in 64% yield.

4b: A white solid in 64% yield; Mp: 64−68 °C, R_f = 0.15 (5:1 *n*-hexane:EtOAc); ^{1}H NMR (400 MHz, $CDCl_3$): δ 7.67 (1H, s), 7.67−7.63 (4H, m), 7.42−7.30 (6H, m), 5.28 (1H, t, J = 7.2 Hz), 5.19 (2H, s), 3.73 (3H, s), 3.40 (2H, d, J = 6.8 Hz), 2.55 (2H, t, J = 6.8 Hz), 2.36 (2H, t, J = 8.0 Hz), 2.14 (3H, s), 1.82 (3H, s), 1.07 (9H, s) ppm; ^{13}C NMR (100 MHz, $CDCl_3$): δ 172.9, 172.5, 163.7, 153.6, 144.0, 135.2, 134.2, 131.9, 129.9, 127.6, 122.5, 122.1, 116.7, 106.3, 70.0, 60.9, 34.7, 29.6, 26.8, 22.6, 19.1, 16.2, 11.5 ppm; HRMS (m/z): calcd for $C_{33}H_{38}O_6SiNa$ $[M + Na]^+$ 581.2335, found: 581.2335.

Synthesis of Triisopropylsilyl (*E*)-6-(4-Hydroxy-6-methoxy-7-methyl-3-oxo-1,3-dihydroisobenzofuran-5-yl)-4-methylhex-4-enoate (4c). To a rapidly stirring solution of MPA **1** (100 mg, 0.3121 mmol) in 0.5 mL of pyridine was added triisopropylsilyl chloride (100 μL, 0.4682 mmol). The reaction mixture was stirred at room temperature for 0.5 h. The crude product was purified by column chromatography (4:1 *n*-hexane:EtOAc) to afford compound **4c** (81.6 mg) as a white solid in 55% yield.

4c: A white solid in 55% yield; Mp: 48−50 °C, R_f = 0.31 (3:1 *n*-hexane:EtOAc); ^{1}H NMR (400 MHz, $CDCl_3$): δ 7.66 (1H, s), 5.24 (1H, t, J = 6.8 Hz), 5.19 (2H, s), 3.76 (3H, s), 3.38 (2H, d, J = 6.8 Hz), 2.43 (2H, t, J = 6.8 Hz), 2.32 (2H, t, J = 8.0 Hz), 2.14 (3H, s), 1.81 (3H, s), 1.04 (3H, m), 1.05−1.00 (18H, m) ppm; ^{13}C NMR (100 MHz, $CDCl_3$): δ 173.4, 172.9, 163.7, 153.7, 144.0, 134.4, 122.3, 122.2, 116.7, 106.4, 70.0, 61.0, 34.8, 34.5, 22.6, 17.7, 16.3, 11.9 ppm; HRMS (m/z): calcd for $C_{26}H_{40}O_6SiNa$ $[M + Na]^+$ 499.2492, found: 499.2489.

General Procedure for the Preparation of Mycophenolate Analogues (5a−5c) and (6b−6c)

To a solution of *tert*-butyldiphenylsilyl ether-MPA product (**3b**) (50 mg, 0.090 mmol) in 1.0 mL of DCM were added DMAP (1.0 mg, 0.0090 mmol) and EDCI (60 mg, 0.3125 mmol) and stirred for 10 min, then alcohol (0.135 mmol) was added to the reaction mixture and allowed to stir at room temperature. After TLC indicated that the reaction was complete, the reaction mixture was diluted with DCM 1.0 mL, quenched with H_2O, extracted with DCM, and washed with brine, the combined organic layers were dried over anhydrous Na_2SO_4 and the solvent was removed by rotary evaporation and purified by column chromatography to obtain product **5**.

To a stirred solution of compound **5** (50 mg) in MeOH 1.0 mL and TBAF (0.02793 mmol) was added at 0 °C and stirred for 30 min. After TLC showed complete conversion of the reaction, the reaction mixture was diluted with 3.0 mL of DCM and quenched with cold saturated NH_4Cl. The reaction mixture was extracted with DCM and washed with brine, followed by drying over Na_2SO_4 anhydrous, and concentrated in vacuo to obtain crude product and purified by column chromatography to afford compound product **6**.

Synthesis of 1,3-Dioxoisoindolin-2-yl (*E*)-6-(4-((*tert*-Butyldiphenylsilyl)oxy)-6-methoxy-7-methyl-3-oxo-1,3-dihydroisobenzofuran-5-yl)-4-methylhex-4-enoate (5a). *N*-Hydroxyphthalimide (22 mg, 0.135 mmol) was added to the reaction mixture and allowed to stir at room temperature for a further 5 h. The crude product was purified by column chromatography (3:1 *n*-hexane:EtOAc) to afford compound **5a** (61.7 mg) as a sticky white oil in 98% yield.

5a: A stricky yellow oil in 98% yield; R_f = 0.30 (3:1 *n*-hexane:EtOAc); ^{1}H NMR (400 MHz, $CDCl_3$): δ 8.90−7.75 (4H, m), 7.70 (4H, d, J = 6.8 Hz), 7.40−7.30 (6H, m), 5.00 (1H, t, J = 6.8 Hz), 4.97 (2H, s), 3.63 (3H, s), 3.18 (2H, d, J = 6.0 Hz), 2.63 (2H, t, J = 7.6 Hz), 2.35 (2H, t, J = 8.0 Hz), 2.12 (3H, s), 1.52 (3H, s), 1.10 (9H, s) ppm; ^{13}C NMR (100 MHz, $CDCl_3$): δ 169.0, 168.2, 163.1, 161.7, 151.4, 145.9, 134.8, 134.6, 133.4, 132.2, 129.3, 128.7, 127.2, 126.8, 124.6, 123.7, 117.7, 111.0, 67.2, 60.4, 33.5, 29.4, 26.3, 24.1, 20.2, 15.8, 11.1 ppm; HRMS (m/z): calcd for $C_{41}H_{41}NO_8SiNa$ $[M + Na]^+$ 726.2499, found: 726.2490.

Synthesis of 4-Fluorophenethyl (*E*)-6-(4-((*tert*-Butyldiphenylsilyl)oxy)-6-methoxy-7-methyl-3-oxo-1,3-dihydroisobenzofuran-5-yl)-4-methylhex-4-enoate (5b). 4-Fluorophenethyl alcohol (17 μL, 0.135 mmol) was added to the reaction mixture and allowed to stir at room temperature for a further 5 h. The crude product was purified by column chromatography (5:1 *n*-hexane:EtOAc) to afford compound **5b** (51.2 mg) as a colorless oil in 84% yield.

5b: A colorless oil in 84% yield; R_f = 0.25 (5:1 *n*-hexane:EtOAc); ^{1}H NMR (400 MHz, $CDCl_3$): δ 7.66 (4H, brs), 7.40−7.25 (6H, m), 7.10 (2H, brs), 6.94 (2H, t, J = 8.4 Hz), 4.95 (1H, brs), 4.88 (2H, s), 4.16 (2H, t, J = 6.4 Hz), 3.60 (3H, s), 3.15 (2H, brs), 2.80 (2H, t, J = 7.2 Hz), 2.26 (2H, t, J = 7.2 Hz), 2.15 (2H, t, J = 6.8 Hz), 2.08 (3H, s), 1.47 (3H, s), 1.07 (9H, s) ppm; ^{13}C NMR (100 MHz, $CDCl_3$): δ 173.0, 168.2, 163.0, 151.4, 134.8, 133.5, 130.1, 129.2, 127.2, 123.5, 117.7, 115.2, 115.0, 111.0, 67.2, 64.5, 60.4, 34.0, 32.7, 26.4, 24.1, 20.2, 16.0, 11.1 ppm; HRMS (m/z): calcd for $C_{41}H_{45}FO_6SiNa$ $[M + Na]^+$ 703.2867, found: 703.2866.

Synthesis of 4-Methoxyphenethyl (*E*)-6-(4-((*tert*-Butyldiphenylsilyl)oxy)-6-methoxy-7-methyl-3-oxo-1,3-dihydroisobenzofuran-5-yl)-4-methylhex-4-enoate (5c). A mixture of *tert*-butyldiphenylsilyl ether-MPA (**3b**) (100 mg, 0.2793 mmol) in 2.0 mL of DCM, DMAP (3.4 mg, 0.02793 mmol), and EDCI (54 mg, 0.2793 mmol) was added and stirred for 10 min, and then, 4-methoxyphenethyl alcohol (64 mg, 0.4190 mmol) was added to the reaction mixture and allowed to stir at room temperature further 24 h. The crude product was purified by column chromatography (5:1 *n*-hexane:EtOAc) to afford compound **5c** (122.7 mg) as a colorless oil in 65% yield.

5c: A colorless oil in 65% yield; R_f = 0.47 (4:1 *n*-hexane:EtOAc); ^{1}H NMR (400 MHz, $CDCl_3$): δ 7.69 (4H, d, J = 9.6 Hz), 7.40−7.24 (6H, m), 7.05 (2H, d, J = 8.4 Hz), 6.80 (2H, t, J = 8.4 Hz), 4.96 (1H, t, J = 6.8 Hz), 4.87 (2H, s), 4.16 (2H, t, J = 7.2 Hz), 3.75 (3H, s), 3.60 (3H, s), 3.16 (2H, d, J = 6.0 Hz), 2.74 (2H, t, J = 7.2 Hz), 2.29 (2H, t, J = 7.2 Hz), 2.16 (2H, t, J = 6.8 Hz), 2.07 (3H, s), 1.48 (3H, s), 1.08 (9H, s) ppm; ^{13}C NMR (100 MHz, $CDCl_3$): δ 173.1, 168.2, 163.0, 158.1, 151.4, 145.8, 134.8, 133.5, 133.4, 129.6, 129.3, 127.2, 127.1, 123.5, 117.7, 113.7, 111.0, 67.2, 64.8, 60.4, 55.1, 34.1, 32.7, 26.4, 24.1, 20.2, 16.0, 11.1 ppm; HRMS (m/z): calcd for $C_{42}H_{48}O_7SiNa$ $[M + Na]^+$ 715.3067, found: 715.3067.

Synthesis of 4-Fluorophenethyl (*E*)-6-(4-Hydroxy-6-methoxy-7-methyl-3-oxo-1,3-dihydroisobenzofuran-5-yl)-4-

https://doi.org/10.1021/acsbiomedchemau.4c00079
ACS Bio Med Chem Au 2025, 5, 106−118

methylhex-4-enoate (6b). A mixture of *tert*-butyldiphenylsilyl ether-MPA (**3b**) (100 mg, 0.2793 mmol) in DCM 2.0 mL, DMAP (3.4 mg, 0.2793 mmol) and EDCI (54 mg, 0.2793 mmol) was added and stirred for 10 min, then 4-fluorophenethyl alcohol (35 μL, 0.2793 mmol) was added to the reaction mixture and allowed to stir at room temperature further 24 h. To a solution of crude product **5b** in MeOH 1.0 mL and TBAF (0.02793 mmol) was added at 0 °C and stirred for 30 min to obtain the crude product **5b**. The crude product **5b** was dissolved in MeOH 1.0 mL and TBAF (73 mg, 0.2793 mmol) was added at 0 °C and continued stirring for 30 min to obtain the crude product **6b**. The crude product **6b** was purified by column chromatography (3:1 *n*-hexane:EtOAc) to afford compound **6b** (62.4 mg) as a yellow oil in 50% yield.

6b: A yellow oil in 50% yield; R_f = 0.24 (3:1 *n*-hexane:EtOAc); ^{1}H NMR (400 MHz, $CDCl_3$): δ 7.66 (1H, brs), 7.12 (2H, q, J = 8.4, 4.8 Hz), 6.96 (2H, t, J = 11.6 Hz), 5.23 (1H, t, J = 7.6 Hz), 5.13 (2H, s), 4.18 (2H, t, J = 7.2 Hz), 3.75 (3H, s), 3.37 (2H, d, J = 7.2 Hz), 2.80 (2H, t, J = 6.8 Hz), 2.38 (2H, t, J = 7.2 Hz), 2.27 (2H, t, J = 6.8 Hz), 2.12 (3H, s), 1.78 (3H, s) ppm; ^{13}C NMR (100 MHz, $CDCl_3$): δ 173.1, 172.8, 163.5, 162.8, 160.3, 153.5, 143.9, 133.9, 133.4, 130.2, 122.6, 122.0, 116.6, 115.2, 115.0, 106.2, 69.9, 64.6, 60.9, 34.4, 34.2, 32.9, 22.5, 16.0, 11.4 ppm; HRMS (m/z): calcd for $C_{25}H_{27}FO_6Na$ $[M + Na]^+$ 465.1689, found: 465.1688.

Synthesis of 4-Methoxyphenethyl (*E*)-6-(4-Hydroxy-6-methoxy-7-methyl-3-oxo-1,3-dihydroisobenzofuran-5-yl)-4-methylhex-4-enoate (6c). The product **5b** (50 mg, 0.072 mmol) was dissolved in 1.0 mL of MeOH, and TBAF (19 mg, 0.072 mmol) was added at 0 °C and continued stirring for 30 min to obtain the crude product of **6b**. The crude product **6b** was purified by column chromatography (3:1 *n*-hexane:EtOAc) to afford compound **6b** (48 mg) as a yellow oil in 99% yield.

6c: A yellow oil in >99% yield; R_f = 0.44 (3:1 *n*-hexane:EtOAc); ^{1}H NMR (400 MHz, $CDCl_3$): δ 7.69 (1H, bs), 7.07 (2H, d, J = 8.4 Hz), 6.82 (2H, d, J = 8.4 Hz), 5.22 (1H, t, J = 7.6 Hz), 5.11 (2H, s), 4.16 (2H, t, J = 7.2 Hz), 3.78 (3H, s), 3.75 (3H, s), 3.37 (2H, d, J = 6.8 Hz), 2.75 (2H, t, J = 7.2 Hz), 2.42−2.35 (2H, m), 2.32−2.25 (2H, m), 2.11 (3H, s) 1.78 (3H, s) ppm; ^{13}C NMR (100 MHz, $CDCl_3$): δ 173.2, 172.9, 163.6, 158.2, 153.6, 144.0, 135.2, 134.1, 129.8, 125.0, 122.6, 122.1, 116.6, 113.9, 106.3, 70.0, 65.0, 61.0, 55.2, 34.6, 34.2, 33.0, 32.2, 26.4, 23.4, 16.1, 11.5 ppm; HRMS (m/z): calcd for $C_{26}H_{30}O_7Na$ $[M + Na]^+$ 477.1889, found: 477.1886.

Synthesis of 1,3-Dioxoisoindolin-2-yl (*E*)-6-(4-Hydroxy-6-methoxy-7-methyl-3-oxo-1,3-dihydroisobenzofuran-5-yl)-4-methylhex-4-enoate (6a). To a solution of MPA **1** (100 mg, 0.3125 mmol) in DCM 2 mL, DMAP (3.8 mg, 0.03125 mmol) and EDCI (60 mg, 0.3125 mmol) were added and stirred for 10 min, then *N*-hydroxyphthalimide (76 mg, 0.4688 mmol) was added to the mixture and allowed to stir at room temperature for a further 5 h. After TLC indicated that the reaction was complete, the reaction mixture was diluted with DCM 3 mL and quenched with H_2O, extracted with DCM and washed with brine, then dried over with Na_2SO_4 anhydrous, and concentrated *in vacuo* to obtain crude product **6a**. The crude product was purified by column chromatography (4:1 *n*-hexane:EtOAc) to afford compound **6a** (46.6 mg) as a yellow solid in 32% yield.

6a: A yellow solid in 32% yield; Mp: 108−110 °C, R_f = 0.59 (1:1 *n*-hexane:EtOAc); ^{1}H NMR (400 MHz, $CDCl_3$): δ 8.90−7.75 (4H, m), 5.33 (1H, t, J = 6.8 Hz), 5.18 (2H, s), 3.76 (3H, s), 3.40 (2H, d, J = 6.8 Hz), 2.74 (2H, t, J = 7.6 Hz), 2.44 (2H, t, J = 8.0 Hz), 2.13 (3H, s), 1.84 (3H, s) ppm; ^{13}C NMR (100 MHz, $CDCl_3$): δ 172.8, 169.1, 163.6, 167.8, 153.5, 144.0, 134.6, 132.8, 128.8, 123.8, 123.7, 121.8, 116.6, 106.3, 69.9, 60.9, 33.9, 29.6, 22.5, 16.0, 11.4 ppm; HRMS (m/z): calcd for $C_{25}H_{23}NO_8Na$ $[M + Na]^+$ 488.1321, found: 488.1317.

■ ASSOCIATED CONTENT

Supporting Information

The Supporting Information is available free of charge at https://pubs.acs.org/doi/10.1021/acsbiomedchemau.4c00079.

^{1}H and ^{13}C NMR spectra (PDF)

■ AUTHOR INFORMATION

Corresponding Authors

Dumnoensun Pruksakorn − *Musculoskeletal Science and Translational Research (MSTR) Center, Faculty of Medicine, Center of Multidisciplinary Technology for Advanced Medicine (CMUTEAM), Faculty of Medicine, and Department of Orthopedics, Faculty of Medicine, Chiang Mai University, Chiang Mai 50200, Thailand*; Email: dumnoensun.p@cmu.ac.th

Rungnapha Saeeng − *Department of Chemistry and Center for Innovation in Chemistry, Faculty of Science and The Research Unit in Synthetic Compounds and Synthetic Analogues from Natural Product for Drug Discovery (RSND), Burapha University, Chonburi 20131, Thailand*; orcid.org/0000-0003-2437-2231; Email: rungnaph@buu.ac.th

Authors

Patamawadee Silalai − *Department of Chemistry and Center for Innovation in Chemistry, Faculty of Science and The Research Unit in Synthetic Compounds and Synthetic Analogues from Natural Product for Drug Discovery (RSND), Burapha University, Chonburi 20131, Thailand*; orcid.org/0009-0004-1534-2668

Pimpisa Teeyakasem − *Musculoskeletal Science and Translational Research (MSTR) Center, Faculty of Medicine and Center of Multidisciplinary Technology for Advanced Medicine (CMUTEAM), Faculty of Medicine, Chiang Mai University, Chiang Mai 50200, Thailand*

Complete contact information is available at: https://pubs.acs.org/10.1021/acsbiomedchemau.4c00079

Author Contributions

CRediT: **Patamawadee Silalai** data curation, investigation, methodology, writing - original draft; **Pimpisa Teeyakasem** investigation; **Dumnoensun Pruksakorn** investigation; **Rungnapha Saeeng** conceptualization, project administration, writing - review & editing.

Notes

The authors declare no competing financial interest.

■ ACKNOWLEDGMENTS

This work was financially supported by (i) Burapha University (BUU), (ii) Thailand Science Research and Innovation (TSRI), (iii) National Science Research and Innovation Fund (NSRF) (Fundamental Fund: Grant no.42/2566), and (iv) the Faculty of Medicine, Chiang Mai University (Grant no. 027/2566), the Research Unit in Synthetic Compounds and Synthetic Analogues from Natural Product for Drug Discovery (RSND) and the Center of Excellence for Innovation in Chemistry (PERCH−CIC). P.S. is grateful for support through the Postdoctoral Fellowship Award from Burapha University. This work was supported by the Science Innovation Facility, Faculty of Science, Burapha University (SIF-IN-42100027).

■ REFERENCES

(1) Chaiyawat, P.; Phanphaisarn, A.; Sirikaew, N.; Klangjorhor, J.; Thepbundit, V.; Teeyakasem, P.; Phinyo, P.; Pruksakorn, D.;

Settakorn, J. IMPDH2 and HPRT expression and a prognostic significance in preoperative and postoperative patients with osteosarcoma. *Sci. Rep.* **2021**, *11*, 10887.
(2) Wang, S. Y.; Hu, H. Z.; Qing, X. C.; Zhang, Z. C.; Shao, Z. W. Recent advances of drug delivery nanocarriers in osteosarcoma treatment. *J. Cancer* **2020**, *11*, 69−82.
(3) Boon, E.; van der Graaf, W. T.; Gelderblom, H.; Tesselaar, M. E.; van Es, R. J.; Oosting, S. F.; de Bree, R.; van Meerten, E.; Hoeben, A.; Smeele, L. E.; Willems, S. M.; Witjes, M. J.; Buter, J.; Baatenburg de Jong, R. J.; Flucke, U. E.; Peer, P. G.; Bovee, J. V.; Van Herpen, C. M. Impact of chemotherapy on the outcome of osteosarcoma of the head and neck in adults. *Head Neck* **2017**, *39*, 140−146.
(4) Debela, D. T.; Muzazu, S. G.; Heraro, K. D.; Ndalama, M. T.; Mesele, B. W.; Haile, D. C.; Kitui, S. K.; Manyazewal, T. New approaches and procedures for cancer treatment: Current perspectives. *SAGE Open Med.* **2021**, *9*, No. 20503121211034366.
(5) Senapati, S.; Mahanta, A. K.; Kumar, S.; Maiti, P. Controlled drug delivery vehicles for cancer treatment and their performance. *Signal Transduct. Target. Ther.* **2018**, *3*, 7.
(6) Silalai, P.; Pruksakorn, D.; Chairoungdua, A.; Suksen, K.; Saeeng, R. Synthesis of propargylamine mycophenolate analogues and their selective cytotoxic activity towards neuroblastoma SH-SY5Y cell line. *Bioorg. Med. Chem. Lett.* **2021**, *45*, No. 128135.
(7) Ardestani, F.; Fatemi, S. S.-a.; Yakhchali, B.; Hosseyni, S. M.; Najafpour, G. Evaluation of mycophenolic acid production by Penicillium brevicompactum MUCL 19011 in batch and continuous submerged cultures. *Biochem. Eng. J.* **2010**, *50*, 99−103.
(8) Regueira, T. B.; Kildegaard, K. R.; Hansen, B. G.; Mortensen, U. H.; Hertweck, C.; Nielsen, J. Molecular basis for mycophenolic acid biosynthesis in Penicillium brevicompactum. *Appl. Environ. Microbiol.* **2011**, *77*, 3035−3043.
(9) Iwaszkiewicz-Grzes, D.; Cholewinski, G.; Kot-Wasik, A.; Trzonkowski, P.; Dzierzbicka, K. Synthesis and biological activity of mycophenolic acid-amino acid derivatives. *Eur. J. Med. Chem.* **2013**, *69*, 863−871.
(10) Ji, Y.; Gu, J.; Makhov, A. M.; Griffith, J. D.; Mitchell, B. S. Regulation of the interaction of inosine monophosphate dehydrogenase with mycophenolic Acid by GTP. *J. Biol. Chem.* **2006**, *281*, 206−212.
(11) Hoffmann, C. V.; Nevez, G.; Moal, M. C.; Quinio, D.; Le Nan, N.; Papon, N.; Bouchara, J. P.; Le Meur, Y.; Le Gal, S. Selection of Pneumocystis jirovecii Inosine 5′-Monophosphate Dehydrogenase Mutants in Solid Organ Transplant Recipients: Implication of Mycophenolic Acid. *J. Fungi (Basel)* **2021**, *7*, 849.
(12) Neuberger, M.; Sommerer, C.; Bohnisch, S.; Metzendorf, N.; Mehrabi, A.; Stremmel, W.; Gotthardt, D.; Zeier, M.; Weiss, K. H.; Rupp, C. Effect of mycophenolic acid on inosine monophosphate dehydrogenase (IMPDH) activity in liver transplant patients. *Clin. Res. Hepatol. Gastroenterol.* **2020**, *44*, 543−550.
(13) Khan, M. S.; Kim, J. S.; Hwang, J.; Choi, Y.; Lee, K.; Kwon, Y.; Jang, J.; Yoon, S.; Yang, C. S.; Choi, J. Effective delivery of mycophenolic acid by oxygen nanobubbles for modulating immunosuppression. *Theranostics* **2020**, *10*, 3892−3904.
(14) Narayanan, M.; Pankewycz, O.; El-Ghoroury, M.; Shihab, F.; Wiland, A.; McCague, K.; Chan, L. Outcomes in African American kidney transplant patients receiving tacrolimus and mycophenolic acid immunosuppression. *Transplantation* **2013**, *95*, 566−572.
(15) Felczak, K.; Vince, R.; Pankiewicz, K. W. NAD-based inhibitors with anticancer potential. *Bioorg. Med. Chem. Lett.* **2014**, *24*, 332−336.
(16) Peitsch, W. K.; Hofmann, I.; Bulkescher, J.; Hergt, M.; Spring, H.; Bleyl, U.; Goerdt, S.; Franke, W. W. Drebrin, an actin-binding, cell-type characteristic protein: induction and localization in epithelial skin tumors and cultured keratinocytes. *J. Invest. Dermatol.* **2005**, *125*, 761−774.
(17) Zheng, Z. H.; Yang, Y.; Lu, X. H.; Zhang, H.; Shui, X. X.; Liu, C.; He, X. B.; Jiang, Q.; Zhao, B. H.; Si, S. Y. Mycophenolic acid induces adipocyte-like differentiation and reversal of malignancy of breast cancer cells partly through PPARgamma. *Eur. J. Pharmacol.* **2011**, *658*, 1−8.
(18) Patel, G.; Thakur, N. S.; Kushwah, V.; Patil, M. D.; Nile, S. H.; Jain, S.; Banerjee, U. C.; Kai, G. Liposomal delivery of mycophenolic acid with quercetin for improved breast cancer therapy in SD rats. *Front. Bioeng. Biotechnol.* **2020**, *8*, 631.
(19) Ramesh, R.; Reddy, D. S. Quest for Novel Chemical Entities through Incorporation of Silicon in Drug Scaffolds. *J. Med. Chem.* **2018**, *61*, 3779−3798.
(20) Grossman, S. A.; Carson, K. A.; Phuphanich, S.; Batchelor, T.; Peereboom, D.; Nabors, L. B.; Lesser, G.; Hausheer, F.; Supko, J. G.; New Approaches to Brain Tumor Therapy CNS Consortium. Phase I and pharmacokinetic study of karenitecin in patients with recurrent malignant gliomas. *Neuro Oncol.* **2008**, *10*, 608−616.
(21) Arnold, S. M.; Rinehart, J. J.; Tsakalozou, E.; Eckardt, J. R.; Fields, S. Z.; Shelton, B. J.; DeSimone, P. A.; Kee, B. K.; Moscow, J. A.; Leggas, M. A phase I study of 7-*t*-butyldimethylsilyl-10-hydroxycamptothecin in adult patients with refractory or metastatic solid malignancies. *Clin. Cancer Res.* **2010**, *16*, 673−680.
(22) Alfthan, O.; Anderson, L.; Esposti, P. L.; Fossa, S. D.; Gammelgaard, P. A.; Gjores, J. A.; Isacson, S.; Rasmussen, F.; Ruutu, M.; Schreeb, T. V.; Setterberg, G.; Strandell, P.; Strindberg, B. Cisobitan in treatment of prostatic cancer. A prospective controlled multicentre study. *Scand. J. Urol. Nephrol.* **1983**, *17* (1), 37−43.
(23) Sirion, U.; Kasemsook, S.; Suksen, K.; Piyachaturawat, P.; Suksamrarn, A.; Saeeng, R. New substituted C-19-andrographolide analogues with potent cytotoxic activities. *Bioorg. Med. Chem. Lett.* **2012**, *22*, 49−52.
(24) Kansom, T.; Sajomsang, W.; Saeeng, R.; Rojanarata, T.; Ngawhirunpat, T.; Patrojanasophon, P.; Opanasopit, P. Fabrication and characterization of andrographolide analogue (3A.1) nanosuspensions stabilized by amphiphilic chitosan derivatives for colorectal cancer therapy. *Drug Delivery Technol.* **2019**, *54*, No. 101287.
(25) Batovska, D. I.; Kim, D. H.; Mitsuhashi, S.; Cho, Y. S.; Kwon, H. J.; Ubukata, M. Hydroxamic acid derivatives of mycophenolic acid inhibit histone deacetylase at the cellular level. *Biosci. Biotechnol.* **2008**, *72*, 2623−2631.
(26) Schwartz, P. A.; Kuzmic, P.; Solowiej, J.; Bergqvist, S.; Bolanos, B.; Almaden, C.; Nagata, A.; Ryan, K.; Feng, J.; Dalvie, D.; Kath, J. C.; Xu, M.; Wani, R.; Murray, B. W. Covalent EGFR inhibitor analysis reveals importance of reversible interactions to potency and mechanisms of drug resistance. *Proc. Natl. Acad. Sci. U. S. A.* **2014**, *111*, 173−178.
(27) Kuzmic, P. DynaFit−a software package for enzymology. *Methods Enzymol* **2009**, *467*, 247−280.
(28) Liu, B.; Gai, K.; Qin, H.; Wang, J.; Liu, X.; Cao, Y.; Lu, Q.; Lu, D.; Chen, D.; Shen, H.; Song, W.; Mei, J.; Wang, X.; Xu, H.; Zhang, Y. Discovery of a Silicon-Containing Pan-Genotype Hepatitis C Virus NS5A Inhibitor. *J. Med. Chem.* **2020**, *63*, 5312−5323.
(29) Liao, L. X.; Song, X. M.; Wang, L. C.; Lv, H. N.; Chen, J. F.; Liu, D.; Fu, G.; Zhao, M. B.; Jiang, Y.; Zeng, K. W.; Tu, P. F. Highly selective inhibition of IMPDH2 provides the basis of antineuroinflammation therapy. *Proc. Natl. Acad. Sci. U. S. A.* **2017**, *114*, E5986−E5994.
(30) Duan, S.; Huang, W.; Liu, X.; Liu, X.; Chen, N.; Xu, Q.; Hu, Y.; Song, W.; Zhou, J. IMPDH2 promotes colorectal cancer progression through activation of the PI3K/AKT/mTOR and PI3K/AKT/FOXO1 signaling pathways. *J. Exp. Clin. Cancer Res.* **2018**, *37*, 304.
(31) Fadaka, A.; Ajiboye, B.; Ojo, O.; Adewale, O.; Olayide, I.; Emuowhochere, R. Biology of glucose metabolization in cancer cells. *J. Oncol. Sci.* **2017**, *3*, 45−51.
(32) Kofuji, S.; Hirayama, A.; Eberhardt, A. O.; Kawaguchi, R.; Sugiura, Y.; Sampetrean, O.; Ikeda, Y.; Warren, M.; Sakamoto, N.; Kitahara, S.; Yoshino, H.; Yamashita, D.; Sumita, K.; Wolfe, K.; Lange, L.; Ikeda, S.; Shimada, H.; Minami, N.; Malhotra, A.; Morioka, S.; Ban, Y.; Asano, M.; Flanary, V. L.; Ramkissoon, A.; Chow, L. M. L.; Kiyokawa, J.; Mashimo, T.; Lucey, G.; Mareninov, S.; Ozawa, T.; Onishi, N.; Okumura, K.; Terakawa, J.; Daikoku, T.; Wise-Draper, T.; Majd, N.; Kofuji, K.; Sasaki, M.; Mori, M.; Kanemura, Y.; Smith, E. P.; Anastasiou, D.; Wakimoto, H.; Holland, E. C.; Yong, W. H.;

https://doi.org/10.1021/acsbiomedchemau.4c00079
ACS Bio Med Chem Au 2025, 5, 106−118

Horbinski, C.; Nakano, I.; DeBerardinis, R. J.; Bachoo, R. M.; Mischel, P. S.; Yasui, W.; Suematsu, M.; Saya, H.; Soga, T.; Grummt, I.; Bierhoff, H.; Sasaki, A. T. IMP dehydrogenase-2 drives aberrant nucleolar activity and promotes tumorigenesis in glioblastoma. *Nat. Cell Biol.* **2019**, *21*, 1003−1014.
(33) Malek, K.; Boosalis, M. S.; Waraska, K.; Mitchell, B. S.; Wright, D. G. Effects of the IMP-dehydrogenase inhibitor, Tiazofurin, in bcr-abl positive acute myelogenous leukemia. Part I. In vivo studies. *Leuk. Res.* **2004**, *28*, 1125−1136.
(34) Villa, E.; Ali, E. S.; Sahu, U.; Ben-Sahra, I. Cancer Cells Tune the Signaling Pathways to Empower de Novo Synthesis of Nucleotides. *Cancers (Basel)* **2019**, *11*, 688.
(35) Roaiah, H. M.; Ghannam, I. A. Y.; Ali, I. H.; El Kerdawy, A. M.; Ali, M. M.; Abbas, S. E.; El-Nakkady, S. S. Design, synthesis, and molecular docking of novel indole scaffold-based VEGFR-2 inhibitors as targeted anticancer agents. *Arch. Pharm.* **2018**, *351*, No. 1700299.
(36) Zhang, Q.; Zheng, P.; Zhu, W. Research Progress of Small Molecule VEGFR/c-Met Inhibitors as Anticancer Agents (2016-Present). *Molecules* **2020**, *25*, 2666.
(37) Wang, R.; Liu, H.; You, Y. Y.; Wang, X. Y.; Lv, B. B.; Cao, L. Q.; Xue, J. Y.; Xu, Y. G.; Shi, L. Discovery of novel VEGFR-2 inhibitors embedding 6,7-dimethoxyquinazoline and diarylamide fragments. *Bioorg. Med. Chem. Lett.* **2021**, *36*, No. 127788.
(38) Assi, T.; Watson, S.; Samra, B.; Rassy, E.; Le Cesne, A.; Italiano, A.; Mir, O. Targeting the VEGF Pathway in Osteosarcoma. *Cells* **2021**, *10*, 1240.
(39) Abdel-Mohsen, H. T.; Abdullaziz, M. A.; Kerdawy, A. M. E.; Ragab, F. A. F.; Flanagan, K. J.; Mahmoud, A. E. E.; Ali, M. M.; Diwani, H. I. E.; Senge, M. O. Targeting Receptor Tyrosine Kinase VEGFR-2 in Hepatocellular Cancer: Rational Design, Synthesis and Biological Evaluation of 1,2-Disubstituted Benzimidazoles. *Molecules* **2020**, *25*, 770.
(40) Jansa, J.; Jorda, R.; Skerlova, J.; Pachl, P.; Perina, M.; Reznickova, E.; Heger, T.; Gucky, T.; Rezacova, P.; Lycka, A.; Krystof, V. Imidazo[1,2-c]pyrimidin-5(6H)-one inhibitors of CDK2: Synthesis, kinase inhibition and co-crystal structure. *Eur. J. Med. Chem.* **2021**, *216*, No. 113309.
(41) El-Naggar, A. M.; El-Hashash, M. A.; Elkaeed, E. B. Eco-friendly sequential one-pot synthesis, molecular docking, and anticancer evaluation of arylidene-hydrazinyl-thiazole derivatives as CDK2 inhibitors. *Bioorg. Chem.* **2021**, *108*, No. 104615.
(42) Li, Y.; Tanaka, K.; Li, X.; Okada, T.; Nakamura, T.; Takasaki, M.; Yamamoto, S.; Oda, Y.; Tsuneyoshi, M.; Iwamoto, Y. Cyclin-dependent kinase inhibitor, flavopiridol, induces apoptosis and inhibits tumor growth in drug-resistant osteosarcoma and Ewing's family tumor cells. *Int. J. Cancer* **2007**, *121*, 1212−1218.
(43) Abdel-Rahman, A. A.; Shaban, A. K. F.; Nassar, I. F.; El-Kady, D. S.; Ismail, N. S. M.; Mahmoud, S. F.; Awad, H. M.; El-Sayed, W. A. Discovery of New Pyrazolopyridine, Furopyridine, and Pyridine Derivatives as CDK2 Inhibitors: Design, Synthesis, Docking Studies, and Anti-Proliferative Activity. *Molecules* **2021**, *26*, 3923.
(44) Galal, A. M. F.; Mohamed, H. S.; Abdel-Aziz, M. M.; Hanna, A. G. Development, synthesis, and biological evaluation of sulfonyl-alpha-l-amino acids as potential anti-Helicobacter pylori and IMPDH inhibitors. *Arch. Pharm.* **2021**, *354*, No. e2000385.
(45) Li, R. J.; Wang, Y. L.; Wang, Q. H.; Wang, J.; Cheng, M. S. In silico design of human IMPDH inhibitors using pharmacophore mapping and molecular docking approaches. *Comput. Math. Methods Med.* **2015**, *2015*, No. 418767.

https://doi.org/10.1021/acsbiomedchemau.4c00079
ACS Bio Med Chem Au 2025, 5, 106−118